THE JOURNAL OF PHYSICAL CHEMISTRY C

ARTICLE

pubs.acs.org/JPCC

Origin of Blue Emission from Silicon Nanoparticles: Direct Transition and Interface Recombination

Shikuan Yang,*[,†] Weizhou Li,[‡] Bingqiang Cao,[§] Haibo Zeng,*[,∥] and Weiping Cai[†]

[†]Key Laboratory of Materials Physics, Anhui Key Laboratory of Nanomaterials and Nanotechnology, Institute of Solid State Physics, Chinese Academy of Sciences, Hefei 230031, People's Republic of China

[‡]School of Materials Science and Engineering, Guangxi University, Nanning, 53004, People's Republic of China

[§]School of Materials Science and Engineering, University of Jinan, Jinan 250022, Shandong, China

[∥]Institute of Nano Science and Key Laboratory of Intelligent Nano Materials and Devices of Ministry of Education, Department of Material Science, Nanjing University of Aeronautics and Astronautics, Nanjing 210016, China

ABSTRACT: Blue light luminescent Si nanoparticles (NPs) have many potential applications in optoelectronics. However, blue light emission from Si is not stable in many cases, which severely hinders their real applications. Here, it is found that Si NPs prepared by laser ablation have strong and aging-enhancement blue light emissions. Subsequent annealing treatment of the aged Si NPs will weaken the blue emission dramatically. Through monitoring the photoluminescence (PL) evolutions (including the peak position and intensity) during different treatments of the Si NPs, we studied the origin of the blue light emission. In this case, such blue light emission cannot be simply ascribed to the quantum confinement effect of Si nanocrystals or surface states. The most plausible luminescent mechanism is that excitons first formed within Si nanocrystals by direct transitions at Γ or *X* point, then some of the formed excitons are trapped by nonradiative Pb centers, and the others transfer to and recombine at near-interface traps located at the interface areas between Si and the surrounding SiO_x ($0 < x < 2$) layer, giving rise to the strong blue light emission. According to this scenario, aging enhancement and annealing reduction of the blue emission could be satisfactorily explained. On the basis of the understanding of the blue light emission mechanism, a time-saving hydrothermal approach is supplied to generate Si NPs with strong blue light emission instead of a time-consuming aging process. This investigation deepens the insight into the mechanism of the blue light emission from Si NPs prepared by laser ablation.

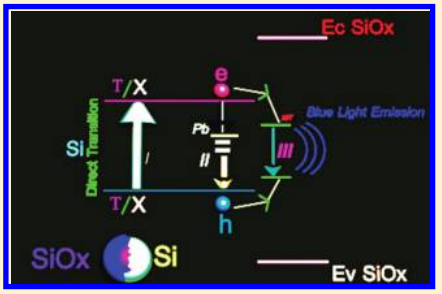

1. INTRODUCTION

Silicon nanoparticles (NPs) with visible light emission have attracted much investigation interest in recent years, due to their potential applications in silicon-based optoelectronics and silicon-based full color display.[1−3] Moreover, the biocompatibility and nontoxicity of Si NPs make them more attractive compared with luminescent II−VI NPs (e.g., CdS, CdSe, which are often highly poisonous) in biotechnological applications such as in cell imaging and biosensors.[4,5] Recent advances in highly efficient light emission from Si NPs with ultrahigh quantum efficiencies (>10%), have spurred more research interest.[6,7] Among the visible light emission, the blue photoluminescence (PL) is always intriguing but a major challenge, especially for the intrinsically indirect and narrow band gap silicon (about 1.1 eV).[8−12]

We have reported that laser ablation in liquid (aqueous solutions or ethanol) can simply and effectively produce Si NPs composed of ultrafine nanocrystals.[13] When ethanol is chosen as the liquid media, narrow size distributed and well-dispersed Si NPs can be prepared.[13] It was further found that Si NPs prepared by laser ablation in liquid can emit blue light.[14] Interestingly, strong aging enhancement of such blue PL was surprisingly observed. It has been reported that the blue PL from Si NPs prepared by other methods sometimes also show aging-enhancement behavior.[15−19] Up to now, the detailed origin of the blue PL from Si NPs has still been controversial. There are at least four main statements associated with the origin of the blue PL from Si NPs: (i) oxide-related defects,[16] (ii) quantum size confinement effect,[18] (iii) quantum size confinement effect combined with surface states,[17,19] and (iv) direction band gap emissions.[20,21] Here, on the basis of various treatments (e.g., aging, annealing, hydrothermal treatment, and rinsing with HF aqueous solution) of the Si NPs prepared by laser ablation and meantime monitoring the PL evolutions (especially the peak shape, location and the intensity), the most plausible origin of the blue PL from Si NPs was supplied. First, excitons form through direct transitions at Γ or *X* point under the excitation light illumination, and then these excitons transfer to and recombine at the near-interface traps residing at the interface regions between the Si nanocrystals and the surrounding silicon oxide. This is a new explanation for the blue emission from Si NPs, which can explain all of the observed phenomena (e.g., aging enhancement, annealing reduction, and stable peak position,

Received: August 8, 2011
Revised: September 29, 2011
Published: October 03, 2011

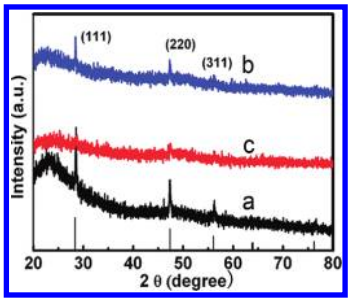

Figure 1. XRD spectra of Si NPs. Curves a−c are related to the as-prepared, heating at 400 and 600 °C for 2 h, respectively.

etc.) in this work. Depending on the mechanism understanding of the blue PL, a simple and time-saving hydrothermal route was provided to generate Si NPs with strong blue PL instead of performing time-consuming aging. This simultaneously consolidated the validity of the supposed blue PL origin from Si NPs.

2. EXPERIMENTAL SECTION

2.1. Preparation of Si NPs. The preparation procedure of the Si NPs is described previously.[13] Briefly, a silicon wafer was ultrasonically rinsed with deionized water and then with ethanol each for 1 h. The cleaned silicon wafer was used as a target, which was immersed in ethanol or deionized water. The irradiation was performed by a Nd:YAG laser operated at 1064 nm with pulse duration of 10 ns and frequency of 10 Hz. The fluence of the laser was maintained at 100 mJ/pulse. The laser beam was focused on the Si target with a spot size about 2 mm in diameter using a lens with a focal length of 150 mm. The solution was continuously stirred during laser irradiation. After irradiation for 30 min, the obtained yellowish solution was centrifuged at 12 000 rounds/min (10 min). The upper transparent liquid was moved away, and then we got the powder products. Annealing treatment was conducted in a horizontal furnace tube.

2.2. Characterizations. The chemical composition and phase structure of the samples were examined by X-ray photoelectron spectroscopy (XPS; ESCALAB 250, Mg Kα) and X-ray diffractometer (XRD; Philips X'Pert) using Cu Kα line (0.154 19 nm), respectively. PL spectra and Fourier transform infrared (FTIR) spectra were measured on the FLS920 PL spectrophotometer with a Xe lamp at room temperature and a NEXUS FTIR spectrometer, respectively. Microstructural examination was conducted on a transmission electron microscope (TEM; JEM-200CX) with 200 kV acceleration voltage by dispersing the powders in ethanol and dropping on a carbon-coated Cu grid. Electronic paramagnetic resonance (EPR) measurements were performed at room temperature on an EPR-200 spectrometer using an *X* band (about 9.65 GHz). The *g* value was calibrated by g_3 and g_4 from Mn^{2+}.

3. RESULTS

3.1. Characterization of the Si NPs. XRD peaks of the as-prepared sample (curve a in Figure 1) can be indexed as a silicon phase with diamond structure (JCPDS card 27-1402). After 400 °C annealing treatment in air, the peak intensity decreases, due to the consumption of some small Si nanocrystals by oxygen (curve b in Figure 1). With further 600 °C treatment, the peaks almost disappear (curve c in Figure 1). TEM observation reveals

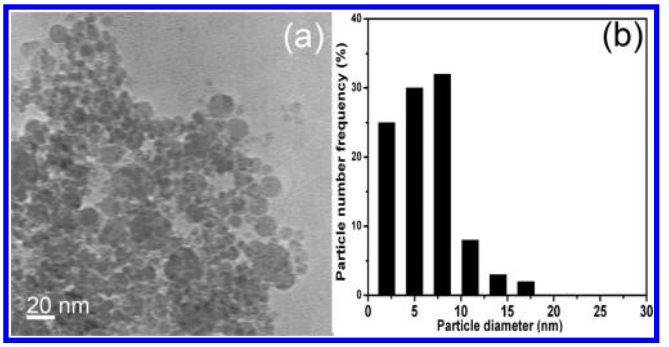

Figure 2. TEM image (a) of the as-prepared Si NPs in ethanol with 100 mJ/pulse laser fluence and the corresponding size distribution (b).

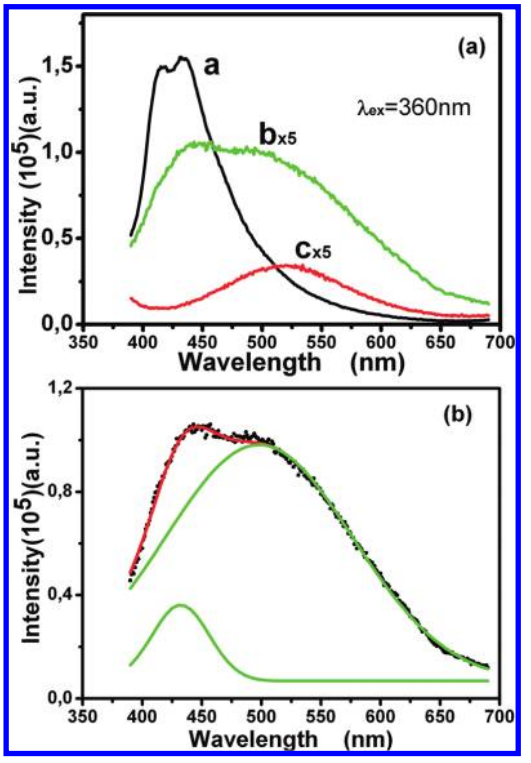

Figure 3. (a) PL spectra of Si NPs from the 4-month-aged (curve a), 400 °C (curve b), and 600 °C (curve c) annealing treated samples (in air). (b) Gaussian-fitting of curve b in panel a.

that the size of the Si nanocrystals ranges from 2 to almost 10 nm (Figure 2). The as-prepared Si NPs show a weak and broad emission band in the violet-blue region with double peaks located at 415 and 435 nm. Subsequent aging will obviously enhance the blue PL emission and keep the peak position unchanged (curve a in Figure 3). After several months aging, the PL intensity is about 2 orders of magnitude higher that that of the fresh sample.[14] The blue PL evolutions during aging and subsequent thermal treatments for the samples prepared in different liquids (e.g., ethanol, deionized water, and different surface surfactant aqueous solutions involving sodium dodecyl sulfate, polyvinylpyrrolidone, and cetyltrimethylammonium bromide) are about in the same manner (results not shown here for clarity). This underlies that the blue PL origin from the Si NPs is independent of the liquid media where they are prepared. For simplicity, here we only show

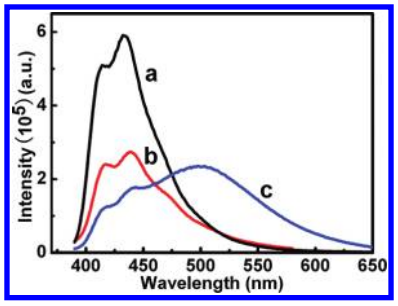

Figure 4. PL spectra from Si NPs prepared with 200 mJ/pulse laser fluence. Curves a−c are related to the sample aged for 4 months and subsequent annealing at 400 and 600 °C for 2 h in air, respectively.

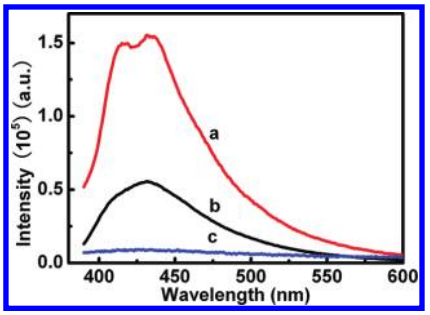

Figure 5. PL spectra from Si NPs aged for 4 months (curve a), subsequently rinsed with 5% HF for 1 h (curve b), and further thermal treatment at 400 °C for 2 h under H_2 protection (curve c).

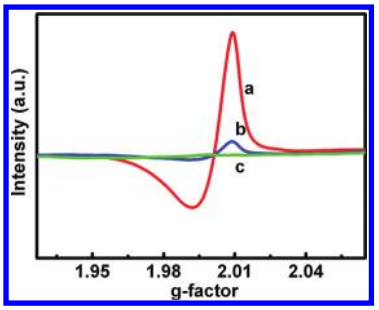

Figure 6. EPR spectra of Si NPs aged for 4 months and further annealing at 400 and 600 °C for 2 h in air, corresponding to curves a−c, respectively.

the PL evolutions of Si NPs prepared in deionized water after different postsynthesis treatment, such as annealing, HF acid rinsing, and hydrothermal treatment.

3.2. PL Measurements. Curve a in Figure 3a exhibits the PL spectrum of the 4-month-aged sample, showing two prominent peaks located at 415 and 435 nm. After annealing the 4-month-aged sample at 400 °C for 2 h, the PL peak broadens (see curve b in Figure 3a). Further analysis reveals that the PL spectrum is composed of two components located at the blue and green region, which can be well-fitted by two Gaussian-type peaks around 430 and 500 nm, as shown in Figure 3b. The blue peak (430 nm) intensity has decreased to about 1/20 compared to that of the sample before the heating treatment. Further annealing at 600 °C (2 h) results in full disappearance of the blue PL component and a new weak peak located at 520 nm emerges (see curve c in Figure 3a). If the annealing treatment is performed in hydrogen gas, after 400 °C for 2 h heating treatment, the Si NPs totally lose the blue PL (curve c in Figure 5).

3.3. Influence of Laser Fluence on the Blue PL Stability. The PL evolution of the Si NPs prepared under different laser fluence is also investigated. It is found that Si NPs prepared with 200 mJ/pulse laser fluence have more stable blue light emission when enduring high-temperature heating treatment, as shown in Figure 4. The 400 °C annealing treatment in air only leads to a little reduced blue PL emission (curve b in Figure 4). Even after 600 °C annealing treatment, the blue PL is still very strong, together with a newly emerged green band situated at about 500 nm (Figure 4, curve c). This phenomenon indicates that Si NPs produced with higher laser fluence have potential applications in blue light emission related devices which needs to operate under high temperatures. On the other hand, after annealing at 600 °C of the Si NPs, the emission band nearly covers the whole visible spectrum and may have applications in silicon-based full color display and white light emitting diodes.

4. DISCUSSION

The Si-NPs' formation mechanism during the laser ablation has been discussed extensively previously.[13,14,22] Here we mainly focus on the origin of the blue PL from the prepared Si NPs by laser ablation in liquid. It should be noted that the origin of the PL from Si nanostructures is highly dependent on the fabrication method.

4.1. Exclusion of the Contribution of SiO_2. SiO_2 often has blue emission when excited by ultrashort wavelength (below 270 nm) instead of 360 nm such as in this study. Furthermore, we have measured the PL of the 4-month-aged sample after 5% HF rinsing, as shown in Figure 5 (see curve b). (HF aqueous solution is effective in removing Si oxidizations. *Caution*! Such solutions are strong corrosives and should be handled carefully.) The blue PL emission does not disappear but only with a little decreased intensity (about 1/3rd that from the 4-month-aged sample, which is mainly caused by the fact that not all of the powers can be collected by centrifugation to do the PL measurement). Additionally, EPR measurements have shown that only one peak at $g = 2.003$ exists, which corresponds to the nonradiative Pb centers caused by silicon dangling bonds (see curve a in Figure 6).[23,24] After annealing treatment, the number of Pb centers decreases and finally below the detection level as shown in curve b and curve c in Figure 6. No other defect-related centers which are often attributed to the blue emission in SiO_2 are detected. Thus, the contribution of the SiO_2 component to the blue PL can be safely excluded.

4.2. Exclusion of the Possibility of Band-to-Band Transition for the Blue PL. On the other hand, we find that the blue PL emission should not be simply ascribed to band-to-band transition within the Si nanocrystals as we previously deemed[14] on the basis of the following experimental results. First, the size reduction of the Si nanocrystals during the annealing treatment without inert gas protection will inevitably take place, and be partially reflected by the Raman shift results shown in Figure 7. The 4-month-aged sample shows a Raman peak shifted to lower wavenumber (curve a in Figure 7) compared to that of bulk silicon (520 cm^{-1}), underlying the existence of ultrafine silicon nanocrystals.[25,26] Subsequent annealing at 400 °C leads to the Raman peak further shifting to lower wavenumber (see curve b in Figure 7), indicating the reduction of the nanocrystal size, and some small ones may be totally consumed. The Raman peak position turns to be nearly the same value as that of the bulk

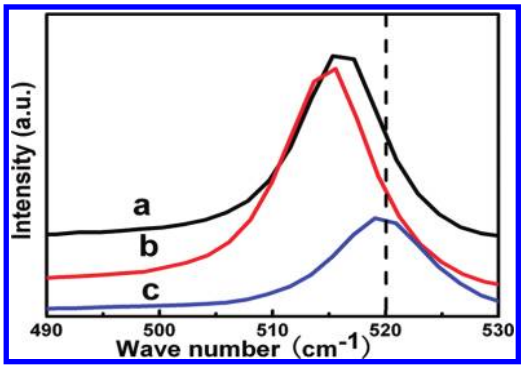

Figure 7. Raman shift spectra of Si NPs aged for 4 months, subsequently annealed at 400 and 600 °C for 2 h in air correspond to curves a−c, respectively. The dashed line is the peak position of the bulk Si at 520 cm^{-1}.

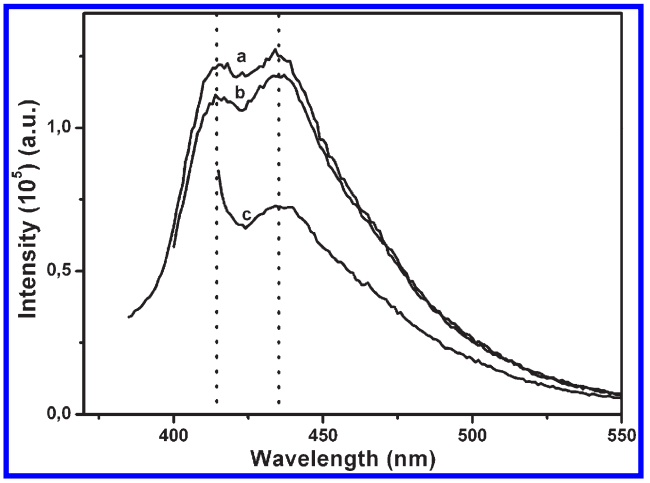

Figure 8. PL spectra of the 4-month-aged Si NPs under different excitation wavelengths. Curves a−c are PL under 360, 380, and 400 nm excitation wavelengths.

silicon after further thermal treatment at 600 °C but with relatively broad full width at half-maximum and asymmetric shape (see curve c in Figure 7), which may be caused by the other factors such as stress force. According to the quantum confinement theory, the band gap widening is closely related to the size of the nanocrystals, whereas the PL peak position does not move as the size of the Si nanocrystals changes caused by the annealing treatment (Figure 3). Moreover, since there is a broad size distribution of the Si nanocrystals (from 2 to about 10 nm, Figure 2), when the excitation wavelength shifts to the red direction, the emission peak should shift to longer wavelength correspondingly due to small sized Si nanocrystals cannot be excited any more if this blue PL really originates from band-to-band recombination within the Si nanocrystals. But experimental results exhibit that as the excitation wavelength shifts from 360 to 380 nm and even further to 400 nm, the PL peak position remains unchanged (Figure 8). The PL intensity evolution is partially caused by the power difference of the excitation light from the Xe lamp at different wavelengths and partly caused by different emission efficiencies under different excitation wavelengths. Moreover, according to the calculations, in order to emit the blue light through the band-to-band recombination, the size of the Si nanocrystals should be less than 2 nm, much smaller

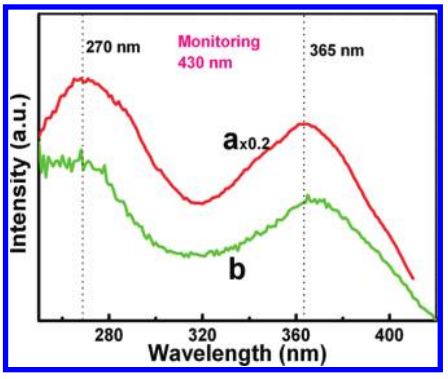

Figure 9. PL excitation spectra of the 4-month-aged Si NPs (curve a) and Si NPs after 400 °C annealing treatment (curve b).

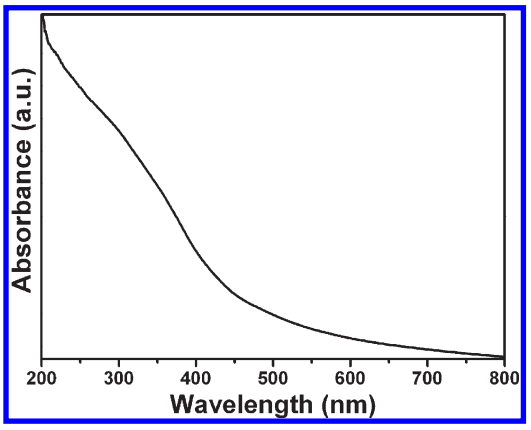

Figure 10. UV−vis absorption spectrum of 4-month-aged Si NPs.

than those prepared in this work. Therefore, the blue PL emission should not simply come from band-to-band recombination within Si nanocrystals.

4.3. Plausible Origin of the Blue PL. *4.3.1. Formation of Excitons by Direct Transition within Si Nanocrystals.* On the basis of the above discussions, the possible origin of the blue PL emission either from the SiO_2 component or from the band-to-band recombination within Si NPs has been safely excluded. PL excitation spectra (curves a and b in Figure 9) demonstrate two excitation peaks at 270 nm (4.5 eV) and 365 nm (3.4 eV) associated with the blue PL emission (monitoring at 430 nm emission). The photon energy of the 365 nm PL excitation peak is in good agreement with the direct transition at the Γ point ($\Gamma_{25} \rightarrow \Gamma_{15}$).[27] The 270 nm (4.5 eV) PL excitation peak is possibly associated with the direction transition at *X* or the $\Gamma_{25} \rightarrow \Gamma_{2'}$ direct transition (energy is 4.2 eV for bulk Si). From the UV−vis absorption spectrum shown in Figure 10, we determine the optical band gap of the Si NPs for an indirect transition to be about 2.3 eV, demonstrating the existence of the quantum confinement effect. According to previous studies, the quantum size confinement will not only influence the indirect band gap but also the direct transition energies such as at the Γ point.[28] The direct $\Gamma_{25} \rightarrow \Gamma_{15}$ transition energy will first increase slightly with the reduction of the Si crystal size and then decrease.[28] Possibly the quantum confinement is attributed to the blue shift of the direct transition at *X* or the $\Gamma_{25} \rightarrow \Gamma_{2'}$ by 0.3 eV from the value of bulk Si. The strong absorption in the <400 nm wavelength region is also reflected in the UV−vis absorption spectrum (Figure 10).

dx.doi.org/10.1021/jp2075836 |*J. Phys. Chem. C* 2011, 115, 21056–21062

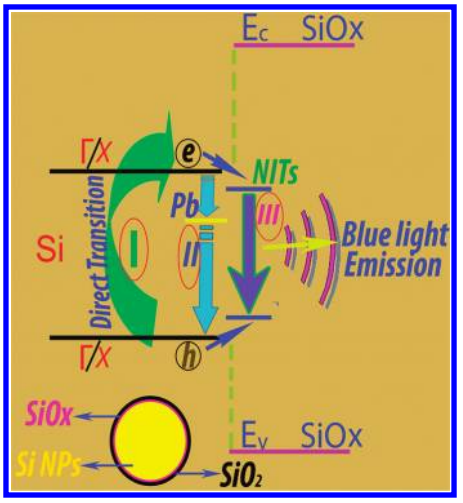

Figure 11. Schematic illustration of the blue PL from Si NPs. Process I: Exciton formation through direction transition. Process II: A few excitons trapped at nonradiative Pb centers. Process III: Transfer of other excitons to NITs and blue light emitted due to recombination. Left-bottom inset: Structure of Si NPs enwrapped by a thin layer of silicon oxide.

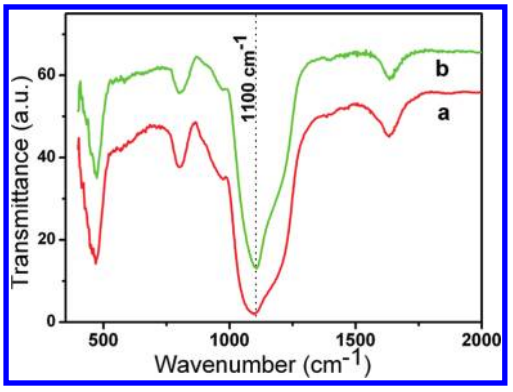

Figure 12. FTIR spectra of the 4-month-aged Si NPs (curve a) and subsequent 400 °C annealing treated Si NPs (curve b).

These results indicate that the blue emission from the Si NPs is caused by the absorption at 365 or 270 nm, corresponding to direct transitions at the Γ or *X* point.

4.3.2. Recombination Pathways of the Excitons. The fate of the photoexcited excitons (electron−hole pairs) in Si is determined by traps and intrinsic recombination processes. Generally, the phonon-assisted indirect band gap electron−hole recombination in Si is very weak.[27,29] Moreover, the optical band gap determined from the UV−vis spectrum (540 nm, 2.3 eV) is far lower than the blue emission (420 nm, 2.95 eV) from the Si NPs. This further consolidates the conclusion that the blue PL of Si NPs is not ascribed to the band-to-band recombination. Consider that Si NPs prepared here are enclosed by a thin SiO_x ($0 < x < 2$) layer (schematically illustrated in the down-left inset image of Figure 11), which has been verified by the XPS results.[14] On the basis of the above analysis, it is proposed that the blue PL emission from Si NPs most probably originates from the following process as schematically illustrated in Figure 11. When quantum sized Si NPs are under excitation light illumination, electrons are excited at the Γ or *X* point (as shown in Figure 11, process I). Some excitons are trapped at nonradiative Pb centers (see Figure 11, process II). The others migrate to the near-interface traps (NITs)[30] residing at the interface regions between Si and SiO_x ($0 < x < 2$)[31−34] and further recombine to emit the blue light (see Figure 11, process III). The strong strain force (caused by the lattice mismatch between the Si nanocrystals and the amorphous silicon oxide) existed near the interface areas between small Si nanocrystals and the surrounding SiO_x ($0 < x < 2$) layer together with the quantum confinement effect must facilitate this kind of recombination process. These NITs tend to be easily passivated by hydrogen, since even when the Si NPs are annealed at relatively lower temperatures (400 °C) in hydrogen gas, the blue PL emission disappears (curve c in Figure 5). Indeed, the detailed information of these NITs still needs further study.

4.3.3. Explanation of the Aging Enhancement of the Blue Emission. As expected, the number of Pb centers should decrease gradually during aging, due to the passivation of Si dangling bonds by oxygen atoms. This process can be proved by the evolution of FTIR spectra from the Si NPs aged for different times.[14] According to the above-mentioned recombination mechanism (Figure 11), the reduction of the number of Pb centers will suppress process II in Figure 11. In the meantime, the luminescent process III in Figure 11 becomes dominant. Therefore, the intensity of the blue PL emission from the Si NPs increased during aging.

4.3.4. Explanation of the Annealing Reduction of the Blue Emission. Subsequent annealing at 400 °C leads to the fact that a large amount of ultrafine Si nanocrystals are consumed (Figure 1) and the number of NITs also decreases, resulting in the restraining of process I and recombination process III in Figure 11. Undoubtedly, such annealing treatment will weaken the blue PL intensity (curve b in Figure 3a). Further thermal treatment at 600 °C gives rise to the disappearance of the NITs, at the same time as the full disappearance of the blue PL (curve c in Figure 3a). Because the blue PL peak position remains unchanged as the Si nanocrystal size changes caused by annealing treatment, the energy state of the NITs should be insensitive to the Si nanocrystal size. They are more dependent on the circumstance near the interface areas between Si NPs and the outlayer SiO_x ($0 < x < 2$) layer. As to the reason why the blue PL emission (Figure 4) from the Si NPs prepared at high laser fluence is comparatively stable even after high-temperature calcination, it is still unclear. It is found that there is a small amount of amorphous Si component in the product confirmed by the Raman shift result (not shown here). The amorphous Si component possibly locates at the outlayer of the Si NPs prepared under higher laser fluence, protecting the inner Si core during the annealing treatment.

4.3.5. Blue PL Peak Splitting. As to why the blue PL emission peak splits into two peaks located at 415 and 435 nm (Figure 3a), we believe that this has a close relationship to the Si−O−Si stretching vibration mode at about 1100 cm^{-1} (Figure 12) in the surrounding silicon oxide layer. The value of 1100 cm^{-1} of the Si−O−Si stretching vibration mode is strikingly close to the splitting distance between the two blue PL peaks. This is further confirmed by the fact that, after the silicon oxide is removed by HF etching, the two PL peaks integrate into one (curve b in Figure 4).

4.3.6. Fast Hydrothermal Way To Enhance the Blue PL. Depending on the understanding of the blue PL emission mechanism from Si NPs stated above, in order to enhance the

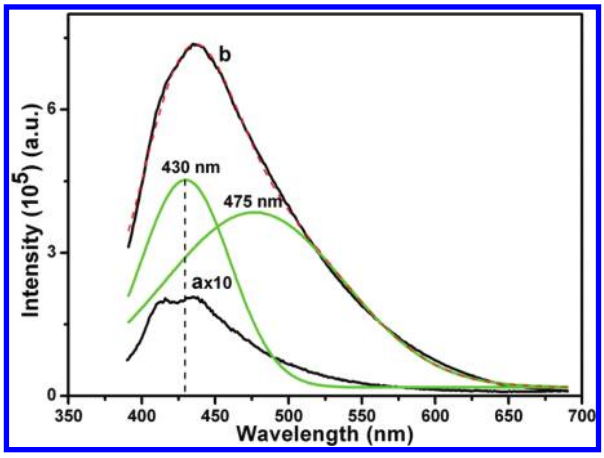

Figure 13. PL spectra from the as-prepared sample (curve a) and after hydrothermal treatment (curve b). Curve b can be well-fitted with two Gaussian-type peaks located at 430 and 475 nm. The red dotted line is fitted peak.

blue PL intensity, the nonradiative process II (Figure 11) must be suppressed and the luminescent process III (Figure 11) must be promoted. To satisfy these two factors, a method which can passivate Si dangling bonds at low temperature is a prerequisite. Si NPs after the PL measurement (curve a in Figure 13) was loaded into a stainless steel autoclave, and then 10 mL of water was added before sealing. It was maintained at 140 °C for 4 h and was cooled naturally. Si powder product was obtained by centrifugation. The morphology and microstructure of the Si NPs after such hydrothermal treatment are nearly unchanged, as verified by TEM, XRD, FTIR, and Raman results (not shown here). However, PL measurement of the Si NPs after the hydrothermal treatment shows an astonishingly strong and wide peak ranging from the blue to the green region (curve b in Figure 13). Further analysis demonstrates that such spectrum can be well-fitted by two Gaussian-type peaks located at 430 and 475 nm. The blue emission from the Si NPs at 430 nm has increased about 20 times compared with that from the Si NPs before the hydrothermal treatment. This blue PL enhancement is obviously attributed to the passivation of Si dangling bonds during the hydrothermal treatment, leading to the decreased number of nonradiative Pb centers, which further results in the depression of the nonradiative process II in Figure 11. On the other hand, the number of Si nanocrystals and NITs are not severely influenced at the relatively low temperature (140 °C). Therefore, blue luminescent process III in Figure 11 is promoted. This method supplies a fast and convenient way to acquire Si NPs with strong blue PL emission instead of through the time-consuming aging route, facilitating their possible applications in optical areas. This result further confirms the blue PL mechanism proposed before (Figure 11). The 475 nm peak may come from SiO_x ($0 < x < 2$) species, which still needs further confirmation.

4.3.7. Origin of the 520 nm PL Emission. As to the origin of the 520 nm PL peak from Si NPs after high-temperature annealing treatment (see curve c in Figure 3a), ref 35 has analyzed this in detail. It is ascribed to the E'_δ centers, which is related with small Si clusters in SiO_2. In our case, annealing is performed in air and the oxidization process will consume the Si component, inevitably giving rise to the formation of small Si clusters and the existence of E'_δ centers. This is further verified by the fact that when the Si NPs are annealed under the hydrogen gas protection, the 520 nm PL peak does not emerge (see curve c in Figure 4).

5. CONCLUSIONS

In summary, it is found that Si NPs prepared by laser ablation in liquid can emit strong blue light. The PL intensity enhances dramatically during the aging process. Subsequent annealing treatment will sharply reduce the blue PL intensity. On the basis of the monitoring of the PL evolutions during various treatments of the Si NPs, we conclude that such blue PL cannot simply be attributed to silicon oxide species or quantum confinement effect of Si nanocrystals. The most plausible mechanism is that excitons first formed inside the quantum sized Si nanocrystals through direction transitions at Γ or X point, and then some of them are caught by nonradiative Pb centers; the others transfer to and recombine at the NITs to emit blue light. On the basis of this mechanism of the blue PL from Si NPs, the aging enhancement and the thermal annealing reduction of the blue PL can be well-explained. Moreover, on the basis of the understanding of the blue PL mechanism from the Si NPs, a hydrothermal route is developed to immediately enhance the PL intensity, instead of by time-consuming aging process, facilitating their applications in optical areas.

AUTHOR INFORMATION

Corresponding Author

*E-mail: skyang@issp.ac.cn. (S.Y.); zeng.haibo.nano@gmail.com (H.Z.).

REFERENCES

(1) Morisaki, H.; Ping, F. W.; One, H.; Yazawa, K. *J. Appl. Phys.* **1991**, *70*, 1869.
(2) Canham, L. T. *Appl. Phys. Lett.* **1990**, *57*, 1046.
(3) Fan, J. Y.; Chu, P. K. *Small* **2010**, *6*, 2080. Shen, P.; Uesawa, N.; Inasawa, S.; Yamaguchi, Y. *J. Mater. Chem.* **2010**, *20*, 1669.
(4) Warner, J. H.; Hoshino, A.; Yamamoto, K.; Tilley, R. D. *Angew. Chem., Int. Ed.* **2005**, *44*, 4550.
(5) Lin, S.-W.; Chen, D.-H. *Small* **2009**, *5*, 72.
(6) Walters, R. J.; Kalkman, J.; Polman, A.; Atwater, H. A.; Dood, de M. J. A. *Phys. Rev. B* **2006**, *73*, 132302.
(7) Jurbergs, D.; Rogojina, E.; Mangolini, L.; Kortshagen, U. *Appl. Phys. Lett.* **2006**, *88*, 233116.
(8) Shirahata, N.; Hasegawa, T.; Sakka, Y.; Tsuruoka, T. *Small* **2010**, *6*, 915.
(9) Rosso-Vasic, M.; Spruijt, E.; van Lagen, B.; Cola, L. D.; Zuilhof, H. *Small* **2008**, *4*, 1835.
(10) Sankaran, R. M.; Holunga, D.; Flagan, R. C.; Giapis, K. P. *Nano Lett.* **2005**, *5*, 537.
(11) Shirahata, N.; Linford, M. R.; Furumi, S.; Pei, L.; Sakka, Y.; Gates, R. J.; Asplund, M. C. *Chem. Commun. (Cambridge, U. K.)* **2009**, 4684. Veinot, J. G. C. *Chem. Commun. (Cambridge, U. K.)* **2006**, 4160.
(12) Heintz, A. S.; Fink, M. J.; Mitchell, B. S. *Adv. Mater.* **2007**, *19*, 3084.
(13) Du, X. W.; Qin, W. J.; Lu, Y. W.; Han, X.; Fu, Y. S.; Hu, S. L. *J. Appl. Phys.* **2007**, *102*, 013518. Yang, S. K.; Cai, W. P.; Zhang, H. W.; Xu, X. X.; Zeng, H. B. *J. Phys. Chem. C* **2009**, *113*, 19091. Zeng, H. B.; Duan, G. T.; Li, Y.; Yang, S. K.; Xu, X. X.; Cai, W. P. *Adv. Funct. Mater.* **2010**, *20*, 561.
(14) Yang, S. K.; Cai, W. P.; Zeng, H. B.; Li, Z. G. *J. Appl. Phys.* **2008**, *104*, 023516. Qin, W. J.; Yang, X. B.; Lu, Y. W.; Sun, J.; Culinich, S. A.; Du, X. W. *Chem. Mater.* **2008**, *20*, 3892.

(15) Hua, F. J.; Drogbogbo, F.; Swihart, M. T.; Ruckenstein, E. *Langmuir* **2006**, *22*, 4263.
(16) Pi, X. D.; Liptak, R. W.; Nowak, J. D.; Wells, N. P.; Carter, C. B.; Campbell, S. A.; Kortshagen, U. *Nanotechnology* **2008**, *19*, 245603.
(17) Portoles, M. J. L.; Nieto, F. R.; Soria, D. B.; Amalvy, J. I.; Peruzzo, P. J.; Martire, D. O.; Kotler, M.; Holub, O.; Gonzalez, M. C. *J. Phys. Chem. C* **2009**, *113*, 13694.
(18) Sercek, V.; Sasaki, T.; Katoh, R.; Shimizu, Y.; Noshizaki, N. *Appl. Phys. B: Lasers Opt.* **2009**, *94*, 133.
(19) Bagabas, A. A.; Gondal, M. A.; Dastageer, M. A.; Al-Muhanna, A. A.; Alanazi, T. H.; Ababtain, M. A. *Nanotechnology* **2009**, *20*, 355703.
(20) Wilcoxon, J. P.; Samara, G. A.; Provencio, P. N. *Phy. Rev. B* **1999**, *60*, 2704.
(21) Zhou, Z.; Brus, L.; Friesner, R. *Nano Lett.* **2003**, *3*, 163.
(22) Zeng, H. B.; Cai, W. P.; Li, Y.; Hu, J. L.; Liu, P. S. *J. Phys. Chem. B* **2005**, *109*, 18260.
(23) Zhang, X. M.; Neiner, D.; Wang, S. Z.; Louie, A. Y.; Kauzlarich, S. M. *Nanotechnology* **2007**, *18*, 095601.
(24) Stesmans, A.; Afanas'ev, V. V. *Appl. Phys. Lett.* **2002**, *80*, 1957. Sato, K.; Hirakuri, K. *J. Appl. Phys.* **2006**, *100*, 114303.
(25) Zi, J.; Zhang, K.; Xie, X. *Phys. Rev. B* **1997**, *55*, 9263.
(26) Paillard, V.; Puech, P.; Laguna, M. A.; Carles, R. *J. Appl. Phys.* **1999**, *86*, 1921.
(27) Wilcoxon, J. P.; Samara, G. A.; Provencio, P. N. *Phys. Rev. B* **1990**, *60*, 2704.
(28) Rama Krishna, M. V.; Friesner, R. A. *J. Chem. Phys.* **1992**, *96*, 873.
(29) Haynes, J. R.; Westphal, W. C. *Phys. Rev.* **1956**, *101*, 1676.
(30) Godefroo, S.; Hayne, M.; Jivanescu, M.; Stesmans, A.; Zacharias, M.; Lebedev, O. I.; Van Tendeloo, G.; Moshchalkov, V. V. *Nat. Nanotechnol.* **2008**, *3*, 174.
(31) Nishikawa, H.; Stahlbush, R. E.; Stathis, J. H. *Phys. Rev. B* **1999**, *60*, 15910.
(32) Puzder, A.; Williamson, A. J.; Grossman, J. C.; Galli, G. *Phys. Rev. Lett.* **2002**, *88*, 097401.
(33) Hadjisavvas, G.; Kelires, P. C. *Phys. Rev. Lett.* **2004**, *93*, 226104.
(34) Averboukh, B.; Huber, R.; Cheah, K. W.; Shen, Y. R.; Qin, G. G.; Ma, Z. C.; Zong, W. H. *J. Appl. Phys.* **2002**, *92*, 3564.
(35) Lin, G.-R.; Lin, C.-J.; Yu, K.-C. *J. Appl. Phys.* **2004**, *96*, 302.